Mini-channel flow condensation enhancement through hydrophobicity in the presence of noncondensable gas

Xi Chen[1], Jordan A. Morrow[1], Melanie M. Derby[1,*]

[1] Department of Mechanical and Nuclear Engineering, Kansas State University,

Manhattan, KS, 66506

[*] Corresponding author
3002 Rathbone Hall, Kansas State University, Manhattan, KS 66506
Telephone: 1 785 532 2606
Fax: 1 785 532 7057

Highlights:

- Condensation at steam mass fluxes of 35– 75 kg/m^{2}s and N_2 mass fractions of 0–30%.
- Nitrogen in hydrophilic channel reduces condensation heat transfer by 24–55%.
- Dropwise condensation heat transfer enhancement in hydrophobic channel with N_2.
- Condensation heat transfer coefficients are a function of vapor mass fraction.

Abstract

Steam condensation is important for a broad range of industrial applications, including power generation and nuclear containment systems. The presence of noncondensable gases in these systems significantly reduces heat transfer, prompting the need for condensation heat transfer enhancement. Steam was condensed in the presence of nitrogen in hydrophilic and hydrophobic 1.82-mm rectangular mini-channels for a range of experimental conditions: steam mass flux (i.e., 35–75 kg/m^{2}s), steam quality (i.e., $0.3 < x < 0.9$), and nitrogen mass fraction (i.e., 0–30%). In the hydrophilic channel, nitrogen mass fractions of 10–30% reduced condensation heat transfer

coefficients by 24–55%. Experimental results were well predicted by the Caruso et al. (2013) correlation. Dropwise condensation was observed in the hydrophobic channel, although the addition of nitrogen suppressed nucleation. In the hydrophobic channel, heat transfer was enhanced by 34–205% over the hydrophilic channel in presence of 10–30% nitrogen, particularly at low vapor mass fractions. Heat transfer coefficients in the hydrophobic channel with 30% nitrogen were identical or higher than those of pure steam in the hydrophilic channel at the same mass flux and quality. Heat transfer coefficients strongly depended on vapor mass fraction, defined as the vapor mass flow rate divided by the three-phase (vapor, liquid and nitrogen) mass flow rate.

Keywords:

Condensation, noncondensable gas, minichannel, wettability, hydrophobicity

1. Introduction

Condensers play an important role in many industrial applications, yet condensation heat transfer performance can be greatly degraded by the presence of noncondensable gases (NCG). Noncondensables, such as air, gather at the liquid-vapor interface and impede condensation heat transfer; in many cases, the thermal resistance across the air becomes the dominant thermal resistance [1-4]. Condensation in the presence of noncondensables is found in many industrial systems, such as thermal desalination units [5], thermosiphons [6], containment systems in nuclear power plants [7], and air-cooled condensers [8]. Further understanding and mitigation of the effects of noncondensable gases on condensation is required.

Based on Nusselt's falling film theory [9], several analytical approaches (e.g. boundary layer method and diffusion layer method) have been employed to understand the impacts of

noncondensable gases on condensation heat transfer. In the boundary layer method, convection in the liquid condensate film and vapor-NCG mixture are solved separately by setting temperature boundary conditions at the liquid-gas interface [1, 10-15]. The diffusion layer method solves heat transfer through three-layer (i.e. vapor gas and liquid) mixture [3, 4, 16-24] in which heat transfer from vapor to liquid through NCG layer is driven by both diffusion and sensible heat transfer caused by vapor partial pressure difference between vapor-NCG and NCG-liquid interfaces. Both methods demonstrate the reduction of condensation heat transfer coefficient with noncondensables.

Minkowycz and Sparrow [1] modeled steam-air mixture condensation on an isothermal vertical plate with laminar free film convection using the boundary layer method. A 0.5% bulk mass fraction of air reduced condensation heat transfer coefficients by up to 50%. Sparrow et al. [10] analytically studied horizontal and vertical flows; at low NCG mass fractions (i.e. 0.5–1%), the effects of NCG on heat flux in horizontal forced flow were negligible while in gravity-driven laminar vertical flows, heat flux was reduced by 80–90%. To investigate the effects of noncondensable gases at wider range of flow conditions and predict heat transfer of practical systems, experiments [25-31] were conducted and empirical correlations were developed using the degradation factor method [16, 25-27] and heat and mass transfer analogy [3, 20, 28-34]. Vierow [25] developed the degradation method, defined as the ratio of experimentally measured condensation heat transfer coefficent with NCG to that of pure steam, typically based on the Nusselt analysis for laminar filmwise condensation heat transfer [35-38]. Lee and Kim [27] developed a degradation factor correlation based on dimensionless shear and NCG mass fraction. Results in showed that the effect of small amount of noncondensables on heat transfer coefficient can be eliminated by reduced channel size (e.g. 3% nitrogen by mass did not significantly affect heat transfer coefficient in the tube of 13-mm inner diameter).

Through analysis and experiments, it has been shown that noncondensables reduce steam condensation heat transfer. Therefore, it is important to consider approaches which could mitigate the effects of noncondensables in condensing systems. Reduced channel size (i.e., mini- and microchannels [39-43] and hydrophobicity [44-48] are two heat transfer enhancement approaches studied in this paper. In mini- and micro-channels, surface tension becomes significant and changes the flow regime to improve heat transfer, and increased surface hydrophobicity promotes dropwise condensation and facilitates liquid removal [48-50]. To understand the influence of steam flow conditions, noncondensable gas fractions, and wettability on condensation heat transfer, this work studies steam condensation heat transfer in 1.82-mm, hydrophilic and hydrophobic rectangular mini-channels at steam mass fluxes of 35–75 kg/m^{2}s, steam qualities of 0.3–0.9, and NCG mass fractions from 0–30%.

2. Experimental method and apparatus

2.1 Experimental apparatus

In order to study the impacts of noncondensables on steam flow condensation, nitrogen was introduced to condensing steam in an open-loop experimental apparatus [48], shown in Figure 1. Steam was sourced from the campus system at 550 kPa, regulated to 250 kPa, and filtered to remove debris. Liquid was removed in the separation tank and the steam superheated 20–30 ^{o}C to determine its enthalpy. Steam was partially condensed in a pre-condenser; in order to conduct an energy balance on the coolant, cooling water mass flow rates were rate measured by a Coriolis flow meter (Micro Motion^{TM} F-series sensor and 2700 transmitter) and inlet and exit temperatures were measured with T-type thermocouples. Ultra-pure nitrogen (mass purity>99.9%, Matheson) was introduced into the system at a pressure 103 kPa higher than the steam pressure to prevent

backflow. Nitrogen volumetric flow rates (Omega^{TM} 7211 rotameter), temperature, and pressure were measured prior to introducing nitrogen between the pre-condenser and test section. Flow stability was monitor visually through the acrylic rotameter, which has a manufacturer-reported full scale uncertainty of 2%. Test section fluid inlet and exit temperatures and pressures were measured; heat transfer measurements and flow visualization could be conducted simultaneously. Following the test section, the steam was fully condensed and its flow rate was determined.

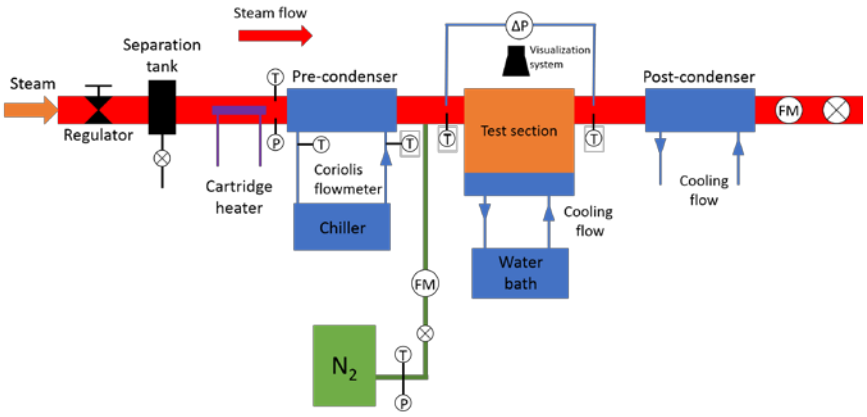

Figure 1 Open-loop flow condensation to study steam flow condensation with injection of nitrogen.

2.2 Test section

The test section simultaneously measured condensation heat transfer coefficients of the steam/liquid/nitrogen mixture and visualized the flow (Figure 2). The mixture entered through an inlet in the PEEK block, entered the oxygen-free copper coupon, and exited through the PEEK block. The 40-mm long, 10-mm wide, and 1-mm deep mini-gap was milled into an oxygen-free copper coupon, resulting in a hydraulic diameter of 1.82 mm. Surface temperature was determined from a near-wall thermocouple 0.5 mm below the channel and heat flux was determined through Heat flux was determined through Fourier's law in the oxygen-free copper block in which five

type T thermocouples were installed in 3.5-mm thermocouple holes spaced 8 mm apart. An indium thermal interface material provided good thermal contact between the coupon and copper block. Due to the three-phase flow (i.e., liquid, vapor, and N_2), fluid temperature was directly measured with a 0.5 mm-diameter thermocouple (TC Direct™ 206-494) inserted into the test section. The test section was cooled via a water bath and low cooling water temperature changes (i.e., < 2 °C) were observed.

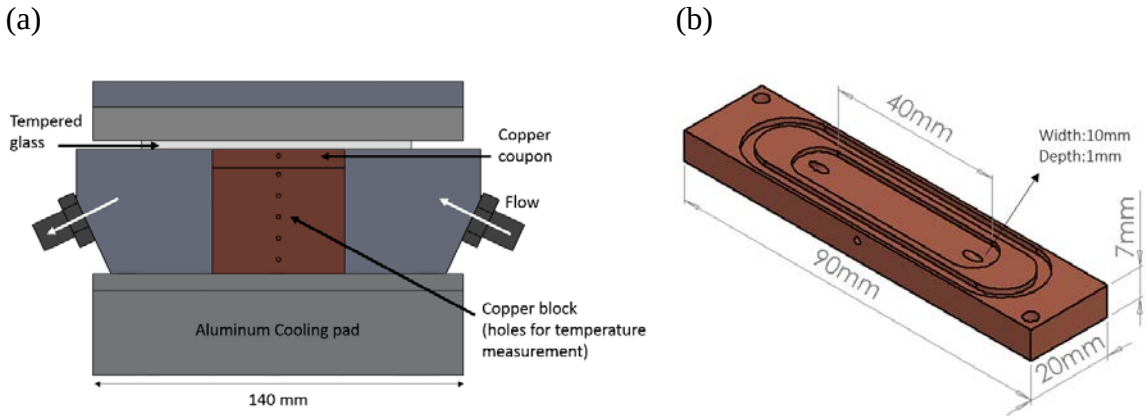

Figure 2 (a) Test section design for visualization and heat transfer measurements and (b) mini-channel coupon.

2.3 Data reduction

Condensation heat transfer coefficients, h, were calculated using Fourier's law to determine heat flux, $q^{"}$,

$$h = \frac{q^{"}}{(T_f - T_w)} = \frac{-k_{cu}\frac{dT}{dy}\frac{A_{block}}{A_{cond}}}{(T_f - T_w)} \quad (1)$$

where T_f and T_w were fluid and wall temperatures, k_{cu} was thermal conductivity of oxygen-free copper, *dT/dy* was the temperature gradient calculated using the least-squares method, and A_{block} and A_{cond} were the areas of the copper block perpendicular to flow, and condensation surface area

in the mini-gap, respectively. The test section inlet quality was determined through an energy balance on the pre-condenser, and the average test section quality, $\bar{x}$, was calculated from inlet quality, x_{in}, and change in quality across the test section Δx_{ts} determined through an energy balance on the copper block.

2.4 Uncertainty analysis

Care was taken to ensure accurate measurements. T-type thermocouples were calibrated in a water bath at seven temperature points in addition to ice and boiling points against a reference thermometer (Omega HH41) with an accuracy of ±0.05 ^{o}C, resulting in a temperature measurement uncertainty of ±0.2 ^{o}C. The uncertainty of temperature gradient in the copper block, $w_{\frac{dT}{dy}}$, was calculated using an equation developed by Kedzierski and Worthington [51],

$$w_{\frac{dT}{dy}} = \sqrt{w_{Ti}^2 + \left(\frac{q"D}{6k_{cu}}\right)^2} \sqrt{\frac{1}{\sum_{i=1}^{N}(y_i - \bar{y})^2}} \tag{2}$$

where w_{Ti} was calibrated thermocouple uncertainty, y_i was distance of the *i*th thermocouple from the condensation surface, and $\bar{y}$ was the average distance of the thermocouple from the condensation surface. Due to the high conductivity of oxygen-free copper, 8-mm spacing between holes, and small diameter of the holes, uncertainties in the temperature gradient uncertainty were low (i.e., less than ± 2%). Pressure transducers were calibrated with a deadweight tester to obtain full range uncertainty of 0.25% (i.e. 2.59 kPa and 0.86 kPa respectively for absolute and differential pressure transducers, respectively). Condensate mass flow rates were measured with an electronic scale, and flow stability was visually monitored with a rotameter at the end of the steam line. Mass flow rate uncertainties contributed minimally to the system uncertainties because

each test lasted more than 10 mins and the flow was very stable (mass flow rate fluctuated less than ± 2%).

The pre-condenser and test section were insulated with fiberglass to prevent ambient heat loss, and the glass window in the test section was insulated during heat transfer data acquisition. The uncertainty in test section steam quality was estimated through a propagation of uncertainty approach. The primary contributor to uncertainty in quality was from the pre-condenser, which is a tube-in-tube heat exchanger. Cooling water entered the pre-condenser at a temperature of 20–35 ^{o}C, and an energy balance was conducted on the coolant. For test purposes, the coolant energy balance was compared to the energy change of fully condensing superheated vapor into single-phase liquid. The cooling side heat transfer rate matched the steam side heat transfer rate within ± 4%. The cooling water flow rate uncertainty contribution was very small due to the accuracy of the Coriolis flow meter, and the steam flow rate uncertainty was negligible due to the stable flow rate and longtime duration. The resultant maximum value in steam quality uncertainty was ± 0.02 and therefore is not shown in the figures. Propagation of uncertainty analysis was conducted using the approach by Kline and McKlintock [52],

$$w_h = \sqrt{\left(\frac{w_{q"_{cond}}}{T_f - T_w}\right)^2 + \left(\frac{w_{T_f}}{(T_f - T_w)^2}\right)^2 + \left(\frac{w_{T_w}}{(T_f - T_w)^2}\right)^2} \quad (3)$$

and heat transfer coefficient uncertainties are plotted in section 3.

2.5 Validation of fluid temperature measurement

In three-phase experiments, fluid temperature of the mixture cannot be predicted from saturation pressure due to the addition of nitrogen. Flow temperature was directly measured with a micro thermocouple inserted to the center point of the channel. Validation tests were conducted for pure steam; fluid temperatures were predicted from pressure drop and the measured micro thermocouple. Condensation heat transfer coefficients were calculated using each fluid temperature. The effects of the thermocouple insertion on condensation heat transfer coefficients were within the experimental uncertainties (Figure 3).

Figure 3 Condensation heat transfer coefficients for pure steam calculated using pressure drop and a micro thermocouple inserted in the channel.

3. Results and discussion

The effects of nitrogen on steam flow condensation were investigated in 1.82-mm mini-channels for various steam mass fluxes, steam qualities, and nitrogen mass fractions in hydrophilic and hydrophobic channels.

3.1 Effects of nitrogen mass fraction, steam mass flux and steam quality in the hydrophilic channel

Liquid-vapor-nitrogen mixtures were condensed for nitrogen mass fractions, ω_N, of 0–30%,

$$\omega_N = \frac{\dot{m}_N}{\dot{m}_{total}} \tag{4}$$

where $\dot{m}_N$ was nitrogen mass flow rate and $\dot{m}_{total}$ was three-phase mixture (i.e. vapor-nitrogen-liquid) flow rate. Higher heat transfer coefficients were observed with increasing steam mass flux, high steam qualities, and low nitrogen mass fractions (Figure 4). The presence of nitrogen decreased condensation heat transfer coefficients by approximately 25–55%. The heat transfer reduction from nitrogen was diminished at lower mass fluxes (i.e. G=35 kg/m^{2}s) and lower steam qualities (i.e. x<0.5). These conditions are associated with lower Reynolds numbers; it is expected that the liquid film thickness is the dominant thermal resistance in these cases, and therefore the thermal resistance from nitrogen is less important. The heat transfer impedance from nitrogen was magnified at high mass fluxes (i.e. G=50 and 75 kg/m^{2}s) and higher steam qualities (i.e. x>0.5) associated higher Reynolds number, where the liquid film thickness was reduced and liquid velocity was increased, thereby reducing the thermal resistance in the liquid phase. Figure 4(d) shows the pressure drop at steam mass flux of 50 kg/m^{2}s and nitrogen mass fraction of 0, 10, 20, and 30%. Increasing nitrogen mass fraction increased pressure drop across the channel by a factor

of up to 5, in part due to increased total flow rate and, therefore, flow velocity and interfacial shear stress. The effects of nitrogen were more significant at high-quality conditions where the addition of nitrogen increased gas-liquid shear. Similar pressure drop behavior was observed at the other two mass fluxes.

(a) (b)

(c) (d)

Figure 4 Condensation heat transfer coefficients at mass fluxes of (a) 35, (b) 50 and (c) 75 kg/m^{2}s and (d) pressure drop at 50 kg/m^{2}s in the hydrophilic channel.

Caruso et al. [5] developed a heat transfer correlation for steam condensation heat transfer in presence of air within slightly inclined (7^o), hydrophilic tubes of 12.6, 20 and 26.8−mm diameters. The correlation was formulated in terms of vapor Nusselt number, Nu_v,

$$\mathrm{Nu_v} = 18.8\mathrm{Re_g^{0.592}Re_l^{-0.13}}\left(\frac{\lambda_\mathrm{N}}{1-\lambda_\mathrm{N}}\right)^{-0.357} \quad (5)$$

where $Re_g = \frac{(\dot{m}_v+\dot{m}_N)D}{\mu_g A}$ and $Re_l = \frac{G(1-x)D}{\mu_l}$ are gas and liquid Reynolds number, respectively, and λ_v is the relative noncondensable mass fraction ($\lambda_\mathrm{N} = \frac{\dot{m}_N}{\dot{m}_g}$). The correlation was fitted from experiments with mixture Reynolds numbers of 500–20,000, NCG mass fraction of 5–42%, and mainly for stratified flow. Results from correlation have been compared with measured condensation mini-channel heat transfer coefficients in the hydrophilic channel (Figure 5). Prediction is excellent, and a 14.5% mean average error is obtained. Although surface tension begins to play important role against gravity in mini-channels, the flow regimes were observed to be stratified flow at low steam qualities (i.e. x < 0.5) and mist flow at high steam qualities (i.e. x >0.5), which are similar to conditions in Caruso et al. [5] correlation.

Figure 5 Experimental heat transfer coefficients predicted with the Caruso et al. [5] correlation.

3.2 Effects of surface wettability on heat transfer, pressure drop and flow regime

In pure steam condensation, increasing surface hydrophobicity promotes dropwise condensation and liquid removal, thereby increasing condensation heat transfer. Heat transfer coefficients in the Teflon-coated, hydrophobic channel (contact angle ~ 107^{o}) are plotted with respect to steam quality in Figure 6. Increased nitrogen reduced heat transfer over the entire steam quality span, similar to hydrophilic channel. However, unlike in hydrophilic channel, lowering steam quality negligibly affected heat transfer coefficients in the hydrophobic channel because liquid formed droplets on hydrophobic surface and facilitating droplet removal, thereby reducing the thermal resistance of the liquid film. Therefore, the enhancement of heat transfer from hydrophobic channel was magnified at low-quality conditions (e.g. $x<0.5$). Although the addition of nitrogen reduced heat transfer coefficients in the hydrophobic channel, dropwise condensation in the channel mitigates the deleterious impacts of nitrogen (Figure 7). For the same steam quality and mass flux, heat transfer coefficients in the hydrophobic channel with 30% mass fraction of nitrogen

were equivalent to or higher than pure steam heat transfer coefficients in the hydrophobic channel. Figure 6b show the pressure drop in both hydrophilic and hydrophilic channel at steam mass flux of 75 kg/m^{2}s and nitrogen mass fraction of 0, 10, 20 and 30%. The hydrophobic channel increased droplet mobility and reduced pressure drop in the channels.

(a) (b)

Figure 6 Comparison of (a) heat transfer and (b) pressure drop in hydrophobic and hydrophilic channels.

Lower surface energies in hydrophobic surfaces promoted dropwise condensation and thus improved removal of condensed liquid. Flow regimes in dropwise condensation differed from those observed in filmwise condensations, including periodic instances of droplet nucleation, coalescence, and departure during dropwise condensation. Figure 7 shows the flow directly before

and after droplets departure at (a) 0%, (b) 10%, and (c) 30% nitrogen mass fractions. Droplet departure diameter decreased with increasing nitrogen mass fraction due to higher interfacial shear stress, but the number of nucleation sites was reduced with increasing nitrogen content. Wider and more frequent rivulet swinging were observed in the presence of nitrogen, which was not favored by heat transfer either. The supplemental videos respectively demonstrate the flow regimes of NCG mass fraction of 0%, 10% and 30% at a steam mass flux of 50 kg/m^{2}s and steam quality of 0.3 in the hydrophobic channel. The playback speed (10 fps) was 1/25 of the real speed (250 fps).

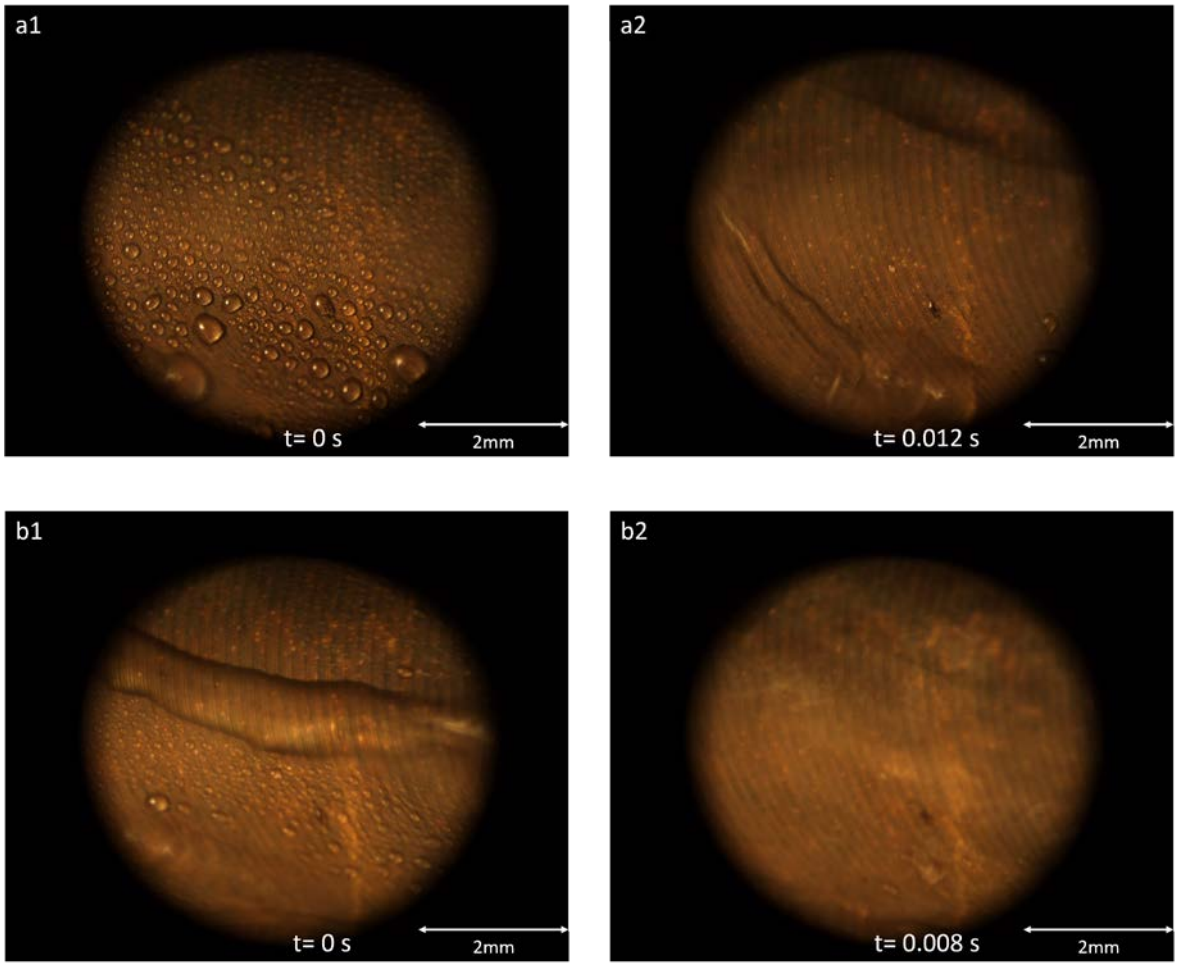

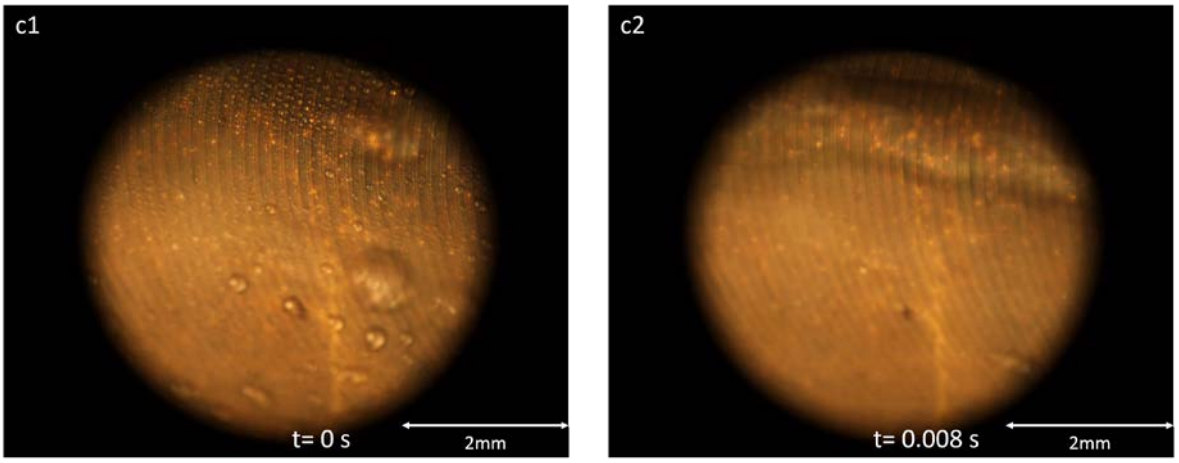

Figure 7 Flow regimes at steam mass flux of 75 kg/m^{2}s and steam quality of 0.3 at nitrogen mass fractions of (a) 0, (b) 10, and (c) 30 %.

3.3 Effects of vapor mass fraction on condensation heat transfer coefficients

Increased steam quality and mass flux, and reduced nitrogen mass fraction, improved condensation heat transfer. Vapor mass fractions, ω_v, were calculated,

$$\omega_v = \frac{\dot{m}_v}{\dot{m}_{total}} = \frac{\dot{m}_v}{\dot{m}_l + \dot{m}_v + \dot{m}_N} \tag{6}$$

where $\dot{m}_v$, is the steam vapor mass flow rate, $\dot{m}_{total}$ is the three-phase mixture mass flow rate.

Vapor mass fraction is a function of both steam quality and nitrogen mass fraction and heat transfer coefficients were found to be a strong function of vapor mass fraction at all flow conditions (Figure 8). Condensation heat transfer coefficients are an increasing function of increased vapor mass fraction for each mass flux and in both hydrophobic and hydrophilic channels. At the same vapor mass fraction, increasing steam mass flux enhanced heat transfer more when the dominant thermal resistances were gas-phase convection and condensation at the vapor-liquid interface instead of

the liquid film resistance. The slope of heat transfer coefficient to vapor mass fraction was less steep in the hydrophobic channel compared to the hydrophilic channel and heat transfer in the hydrophobic channel was less sensitive to the effects of decreasing steam quality and increasing nitrogen mass fraction.

Figure 8 Condensation heat transfer coefficient behavior with mass fraction of vapor.

4. Conclusions

- Steam flow condensation in presence of NCG was studied in an open-loop system with variable steam mass fluxes (i.e., 35–75 kg/m^{2}s), steam qualities (i.e., 0.3–0.9), nitrogen mass fractions (i.e., 0–35%) in hydrophilic and hydrophobic 1.82-mm mini-gaps.
- Higher heat transfer coefficients were observed at higher steam mass fluxes, steam qualities, and lower nitrogen mass fractions. Enhancements were more pronounced when the dominant thermal resistances were at the vapor-liquid interface and in vapor phase.

- Surface hydrophobicity in the hydrophobic channel increased heat transfer coefficients to values yields more significant enhancement at low-quality conditions where the dominant thermal resistance lies in the liquid phase.
- Pressure drops in the channel have been lifted by increased steam mass flux, steam quality and increased NCG mass fraction for increased interfacial velocity and therefore increased interfacial shear stress and have been reduced by channel hydrophobicity for lower surface energy induced lower liquid-solid friction.
- Flow regime on hydrophobic surfaces with mass flux of 50 kg/m^{2}s, steam quality of 0.5 and NCG mass flux of 0, 10, and 30% have been captured. Reduced droplet departure size and nucleation sites are found.
- Comparing experimental results in hydrophilic channel with Caruso et al. (2013) correlations great agreement with an MAE of 14.5% is obtained, indicating a nice predictive tool for condensation heat transfer coefficient in a hydrophilic channel of 1.82-mm rectangular

5. Acknowledgements

We gratefully acknowledge the partial support of the Electrical Power Affiliates Program.

Nomenclature

A	Area (m^2)
C	Flow-based constant
Cp	Specific heat (kJ/kgK)
D	Diameter (m)
F	Heat transfer coefficient degradation factor

h	Heat transfer coefficient (W/m^2K)
i	Evaporative enthalpy (kJ/kg)
k	Thermal conductivity (W/mK)
$\dot{m}$	Mass flow rate (kg/s)
Nu	Nusselt number
P	Pressure (kPa)
P_{red}	Reduced pressure
$\dot{Q}$	Heat transfer rate (W)
q”	Heat flux (W/m^2)
Re_l	Liquid Reynolds number $Re_l = \frac{G(1-x)D}{\mu_l}$
Re_v	Vapor Reynolds number $Re_v = \frac{GxD}{\mu_v}$
Re_g	Gas Reynolds number $Re_g = \frac{(\dot{m}_v+\dot{m}_N)D}{\mu_g A}$
Sc	Schmidt number
T	Temperature (K)
$\dot{V}$	Volumetric flow rate (m^3/s)
w	Uncertainty
x	Steam quality
y	Vertical distance from the condensation surface (m)

Greek letters:

ρ	Density (kg/m^3)
λ	Relative mass fraction
ω	Mass fraction in vapor-nitrogen-liquid mixture

Subscript:

cond	Condensation
exp	Experiment
f	Flow
fg	liquid-vapor phase change

g	Gas (including vapor and nitrogen)
l	Liquid
N	Nitrogen
pre	Prediction
st	Steam
ts	Test section
v	vapor
w	wall

References

1. Minkowycz, W. and E. Sparrow, *Condensation heat transfer in the presence of noncondensables, interfacial resistance, superheating, variable properties, and diffusion.* International Journal of Heat and Mass Transfer, 1966. **9**(10): p. 1125-1144.

2. Denny, V., A. Mills, and V. Jusionis, *Laminar film condensation from a steam-air mixture undergoing forced flow down a vertical surface.* Journal of Heat Transfer, 1971. **93**(3): p. 297-304.

3. Colburn, A.P. and O.A. Hougen, *Studies in Heat Transmission1I—Measurement of Fluid and Surface Temperatures.* Industrial & Engineering Chemistry, 1930. **22**(5): p. 522-524.

4. Peterson, P., V. Schrock, and T. Kageyama, *Diffusion layer theory for turbulent vapor condensation with noncondensable gases.* Journal of Heat Transfer, 1993. **115**(4): p. 998-1003.

5. Caruso, G., D.V. Di Maio, and A. Naviglio, *Condensation heat transfer coefficient with noncondensable gases inside near horizontal tubes.* Desalination, 2013. **309**: p. 247-253.

6. Mantelli, M.B.H., W.B. Ângelo, and T. Borges, *Performance of naphthalene thermosyphons with non-condensable gases–Theoretical study and comparison with data.* International Journal of Heat and Mass Transfer, 2010. **53**(17): p. 3414-3428.

7. Xu, H., et al., *Experimental study on the effect of wall-subcooling on condensation heat transfer in the presence of noncondensable gases in a horizontal tube.* Annals of Nuclear Energy, 2016. **90**: p. 9-21.

8. Bustamante, J.G., A.S. Rattner, and S. Garimella, *Achieving near-water-cooled power plant performance with air-cooled condensers.* Applied Thermal Engineering, 2015.

9. Nusselt, W., *Die Oberflachenkondesation des Wasserdamffes the surface condensation of water.* Zetrschr. Ver. Deutch. Ing., 1916. **60**: p. 541-546.

10. Sparrow, E., W. Minkowycz, and M. Saddy, *Forced convection condensation in the presence of noncondensables and interfacial resistance.* International Journal of Heat and Mass Transfer, 1967. **10**(12): p. 1829-1845.

11. Sparrow, E. and S. Lin, *Condensation heat transfer in the presence of a noncondensable gas.* Journal of Heat Transfer, 1964. **86**(3): p. 430-436.

12. Sparrow, E. and E. Eckert, *Effects of superheated vapor and noncondensable gases on laminar film condensation.* AIChE Journal, 1961. **7**(3): p. 473-477.

13. Rose, J., *Condensation of a vapour in the presence of a non-condensing gas.* International Journal of Heat and Mass Transfer, 1969. **12**(2): p. 233-237.

14. Rose, J., *Approximate equations for forced-convection condensation in the presence of a non-condensing gas on a flat plate and horizontal tube.* International Journal of Heat and Mass Transfer, 1980. **23**(4): p. 539-546.

15. Tang, G., et al., *Film condensation heat transfer on a horizontal tube in presence of a noncondensable gas.* Applied Thermal Engineering, 2012. **36**: p. 414-425.

16. Vierow, K. and V. Schrock. *Condensation in a natural circulation loop with noncondensable gases, 1*. in *Proceedings of the international conference on multiphase flows' 91-Tsukuba*. 1991.

17. Kageyama, T., P. Peterson, and V. Schrock, *Diffusion layer modeling for condensation in vertical tubes with noncondensable gases.* Nuclear engineering and design, 1993. **141**(1): p. 289-302.

18. Peterson, P.F., *Diffusion layer modeling for condensation with multicomponent noncondensable gases.* Journal of heat transfer, 2000. **122**(4): p. 716-720.

19. Ogg, D.G., *Vertical downflow condensation heat transfer in gas-steam mixtures*. 1991: University of California, Berkeley.

20. Munoz-Cobo, J., et al., *Turbulent vapor condensation with noncondensable gases in vertical tubes.* International journal of heat and mass transfer, 1996. **39**(15): p. 3249-3260.

21. Revankar, S.T. and D. Pollock, *Laminar film condensation in a vertical tube in the presence of noncondensable gas.* Applied Mathematical Modelling, 2005. **29**(4): p. 341-359.

22. Brouwers, H., *Effect of fog formation on turbulent vapor condensation with noncondensable gases.* Journal of heat transfer, 1996. **118**(1): p. 243-245.

23. Liao, Y. and K. Vierow, *A generalized diffusion layer model for condensation of vapor with noncondensable gases.* Journal of Heat Transfer, 2007. **129**(8): p. 988-994.

24. Liao, Y., et al., *Transition from natural to mixed convection for steam–gas flow condensing along a vertical plate.* International Journal of Heat and Mass Transfer, 2009. **52**(1): p. 366-375.

25. Vierow, K.M., *Behavior of steam-air systems condensing in cocurrent vertical downflow*. 1990: University of California, Berkeley.

26. Kuhn, S., V. Schrock, and P. Peterson, *An investigation of condensation from steam–gas mixtures flowing downward inside a vertical tube.* Nuclear Engineering and Design, 1997. **177**(1): p. 53-69.

27. Lee, K.-Y. and M.H. Kim, *Experimental and empirical study of steam condensation heat transfer with a noncondensable gas in a small-diameter vertical tube.* Nuclear Engineering and Design, 2008. **238**(1): p. 207-216.

28. Oh, S. and S.T. Revankar, *Experimental and theoretical investigation of film condensation with noncondensable gas.* International Journal of Heat and Mass Transfer, 2006. **49**(15): p. 2523-2534.

29. Blangetti, F., R. Krebs, and E. Schlunder, *Condensation in vertical tubes-experimental results and modeling.* Chemical Engineering Fundamentals, 1982. **1**(1): p. 20-63.

30. Maheshwari, N., et al., *Investigation on condensation in presence of a noncondensable gas for a wide range of Reynolds number.* Nuclear Engineering and Design, 2004. **227**(2): p. 219-238.

31. Chantana, C. and S. Kumar, *Experimental and theoretical investigation of air-steam condensation in a vertical tube at low inlet steam fractions.* Applied Thermal Engineering, 2013. **54**(2): p. 399-412.

32. Wallis, G.B., *One-dimensional two-phase flow*. 1969: McGraw-Hill Companies.

33. No, H.C. and H.S. Park, *Non-iterative condensation modeling for steam condensation with non-condensable gas in a vertical tube.* International Journal of Heat and Mass Transfer, 2002. **45**(4): p. 845-854.

34. Liao, Y., et al., *Reflux condensation of flowing vapor and non-condensable gases counter-current to laminar liquid film in a vertical tube.* Nuclear Engineering and Design, 2009. **239**(11): p. 2409-2416.

35. Chen, S., F. Gerner, and C. Tien, *General film condensation correlations.* Experimental Heat Transfer An International Journal, 1987. **1**(2): p. 93-107.

36. Chen, M.M., *An analytical study of laminar film condensation: part 1—flat plates.* Journal of heat transfer, 1961. **83**(1): p. 48-54.

37. Koh, J., E. Sparrow, and J. Hartnett, *The two phase boundary layer in laminar film condensation.* International Journal of Heat and Mass Transfer, 1961. **2**(1-2): p. 69-82.

38. Koh, J., *Laminar film condensation of condensable gases and gaseous mixtures on a flat plate.* Proc 4th USA Nat Cong Appl Mech, 1962. **2**: p. 1327-1336.

39. Shin, J.S. and M.H. Kim, *An experimental study of flow condensation heat transfer inside circular and rectangular mini-channels.* Heat transfer engineering, 2005. **26**(3): p. 36-44.

40. Fang, C., et al., *Influence of film thickness and cross-sectional geometry on hydrophilic microchannel condensation.* International Journal of Multiphase Flow, 2010. **36**(8): p. 608-619.

41. Agarwal, A. and S. Garimella, *Representative Results for Condensation Measurements at Hydraulic Diameters ~ 100 Microns.* Journal of Heat Transfer, 2010. **132**(4): p. 041010.

42. Bandhauer, T.M., A. Agarwal, and S. Garimella, *Measurement and modeling of condensation heat transfer coefficients in circular microchannels.* Journal of Heat Transfer, 2006. **128**(10): p. 1050-1059.

43. Webb, R.L. and K. Ermis, *Effect of hydraulic diameter on condensation of R-134a in flat, extruded aluminum tubes.* Journal of Enhanced Heat Transfer, 2001. **8**(2).

44. Baojin, Q., et al., *Experimental study on condensation heat transfer of steam on vertical titanium plates with different surface energies.* Experimental Thermal and Fluid Science, 2011. **35**(1): p. 211-218.

45. Bonner, R.W. *Dropwise condensation life testing of self assembled monolayers*. in *2010 14th International Heat Transfer Conference*. 2010: American Society of Mechanical Engineers.

46. Vemuri, S. and K. Kim, *An experimental and theoretical study on the concept of dropwise condensation.* International Journal of Heat and Mass Transfer, 2006. **49**(3): p. 649-657.

47. Derby, M.M., et al., *Flow condensation heat transfer enhancement in a mini-channel with hydrophobic and hydrophilic patterns.* International Journal of Heat and Mass Transfer, 2014. **68**: p. 151-160.

48. Chen, X. and M.M. Derby, *Combined visualization and heat transfer measurements for steam flow condensation in hydrophilic and hydrophobic mini-gaps.* Journal of Heat Transfer, 2016. **138**(9): p. 091503.

49. Ma, X.-H., et al., *Condensation heat transfer enhancement in the presence of non-condensable gas using the interfacial effect of dropwise condensation.* International Journal of Heat and Mass Transfer, 2008. **51**(7): p. 1728-1737.

50. Rose, J., *Surface tension effects and enhancement of condensation heat transfer.* Chemical Engineering Research and Design, 2004. **82**(4): p. 419-429.

51. Kedzierski, M. and J. Worthington III, *Design and machining of copper specimens with micro holes for accurate heat transfer measurements.* Experimental Heat Transfer, 1993. **6**(4): p. 329-344.

52. Kline, S.J. and F. McClintock, *Describing uncertainties in single-sample experiments.* Mechanical engineering, 1953. **75**(1): p. 3-8.